

Guilherme Nader-Marta¹, Sachin Kumar Deshmukh², Kristina Fanucci¹, Adrian V. Lee³, Steffi Oesterreich³, Sharon Wu², Joanne Xiu², Pooja Prem Advani⁴, Priscila Barreto Coelho⁵, Maryam B. Lustberg⁶, Stuart J. Schnitt⁷, Nancy U. Lin¹, Sara M. Tolaney¹, Erica L. Mayer¹, Otto Metzger¹, George W. Sledge Jr², Rinath Jeselsohn¹

1. Dana-Farber Cancer Institute, Harvard Medical School, Boston, MA; 2. Caris Life Sciences, Phoenix, AZ; 3. UPMC Hillman Cancer Center, University of Pittsburgh, Pittsburgh, PA; 4. Mayo Clinic, Jacksonville, FL; 5. Sylvester Comprehensive Cancer Center, University of Miami, Miami, FL; 6. Yale Cancer Center, Yale School of Medicine, New Haven, CT; 7. Beth Israel Deaconess Medical Center, Boston, MA;

BACKGROUND

- Invasive lobular carcinoma (ILC) is a distinct breast cancer (BC) subtype with dissemination patterns differing from invasive breast carcinoma of no special type (BC-NST).¹
- While genomic differences between ILC and BC-NST have been described^{2,3}, the extent to which molecular and immune profiles vary by metastatic organ and histology is poorly characterized.

METHODS

Study Design and Data Source

- Retrospective analysis of de-identified tumor samples from patients with metastatic breast cancer (mBC) profiled at Caris Life Sciences (Phoenix, AZ), a CLIA/CAP-certified laboratory.

Patient Selection

- Patients with mBC who underwent next-generation sequencing. Histology was restricted to pure ILC or BC-NST.
- Samples derived from metastatic lesions or breast lesions obtained after diagnosis of metastatic disease (Table 1).

Table 1. Distribution of Specimen Site Counts

Specimen Site	BC-NST (N)	ILC (N)
Skin	785	172
Lymph node	401	84
Bone	109	62
Breast	361	56
GI tract (GI)	5	56
Liver	220	54
Female genital tract	10	43
Peritoneum	15	37
CNS	44	11
Lung	77	9

Molecular Profiling

- DNA sequencing was performed using a 592-gene panel.
- Whole-transcriptome sequencing (WTS) was performed for gene expression analyses.
- Variants classified per ACMG guidelines; pathogenic and likely pathogenic alterations included.
- Immune cell proportions estimated using transcriptomic deconvolution (quanTIseq).

Statistical Analysis

- Comparisons performed: (1) Within histology and (2) Across histologies (ILC vs BC-NST)
- Statistical tests: Chi-square for categorical variables, Mann-Whitney U test for continuous variables
- Multiple testing correction using false discovery rate (FDR) $q < 0.05$ considered statistically significant

RESULTS

Mutation and Amplification Frequency

- In ILC, *ERBB2* mut frequency differed by metastatic site ($q < 0.01$), with higher prevalence in the liver (32.7%) and lower in gastrointestinal (GI) lesions (3.7%), $q < 0.05$, (Figure 1).
- In BC-NST, *ESR1* mutation (Figure 2) and *GATA3* mutation (Figure 3) and *FGFR1* amplification (Figure 4) were enriched in liver metastases (*ESR1*: 28.2%, *GATA3*: 17.8%, *FGFR1*: 16.5%), $q < 0.05$.
- No organ-specific differences were observed in either histology for *PIK3CA*, *AKT*, *PTEN*, *BRCA1*, *BRCA2* or *RB1*.

Fig 1. ERBB2 Mutation Frequency by Metastatic Site

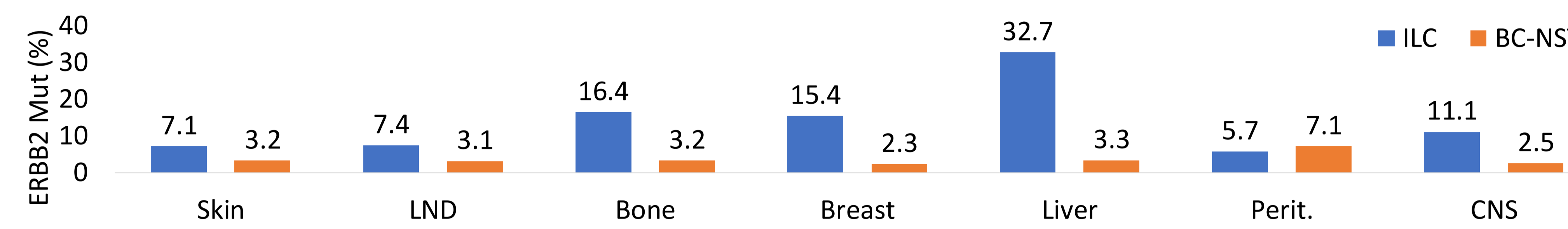


Fig 2. ESR1 Mutation Frequency by Metastatic Site

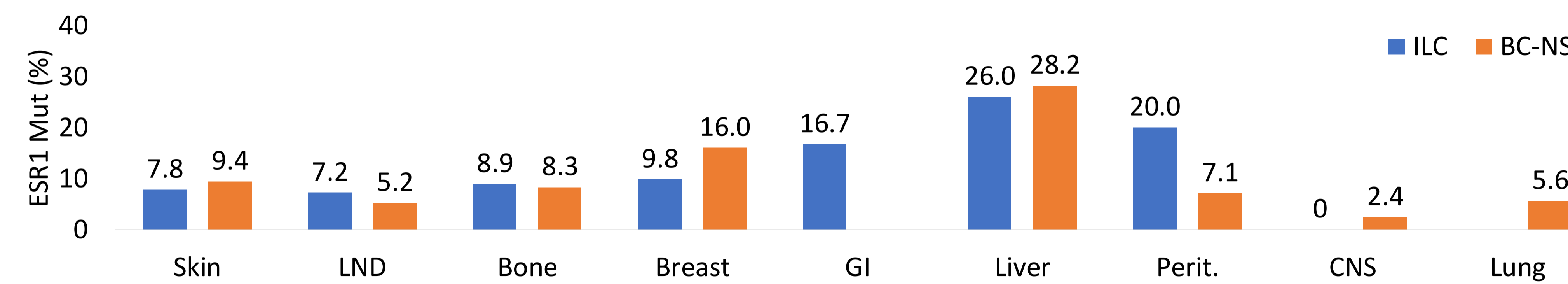


Fig 3. GATA3 Mutation Frequency by Metastatic Site

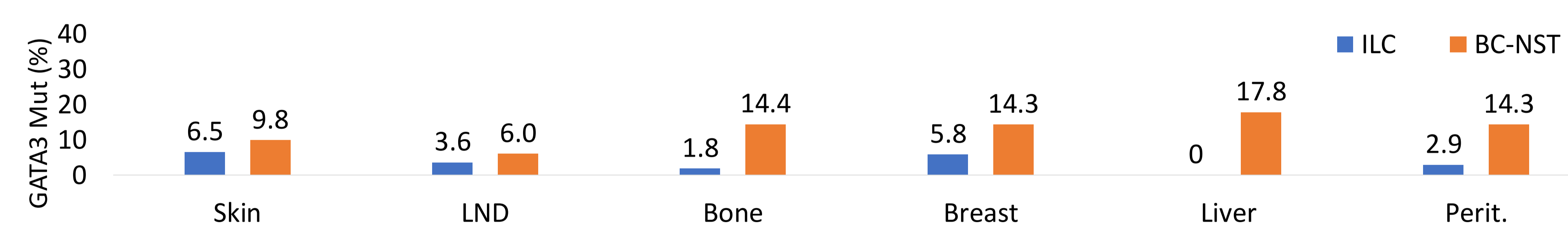
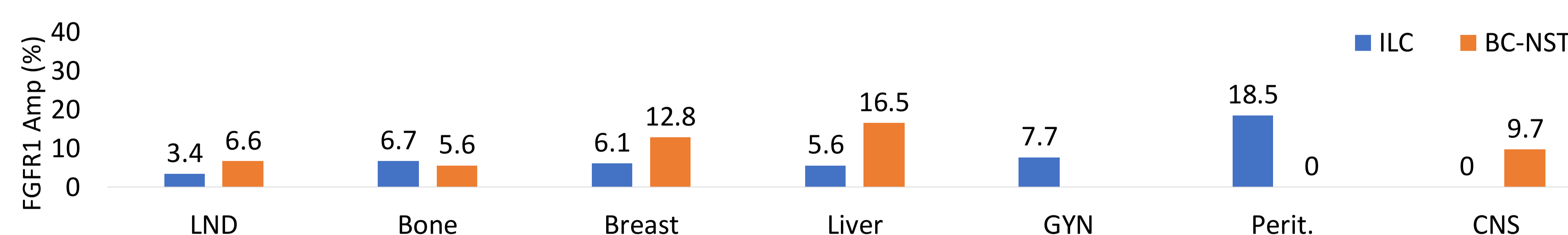


Fig 4. FGFR1 Amplification Frequency by Metastatic Site



PD-L1 Positivity

- In BC-NST, PD-L1 IHC protein expression was highest in skin (20.7%) and lowest in liver (5.0%) ($q = 0.02$) (Figure 5).
- There was no difference in PD-L1 positivity within ILC metastatic sites (Figure 6)

Figure 5. PD-L1 positivity BC-NST metastatic site

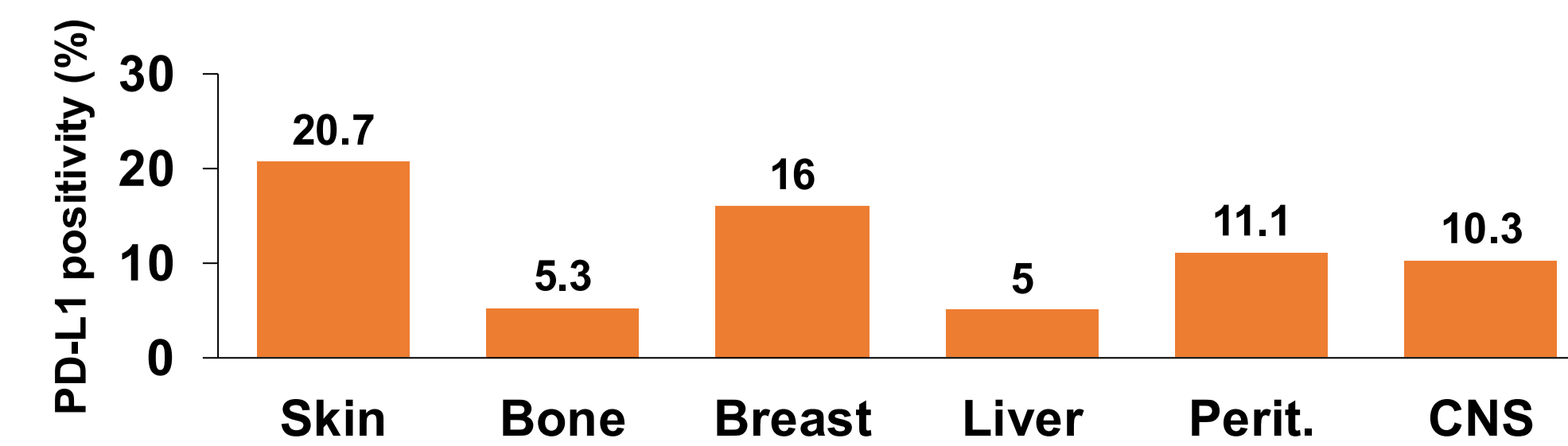
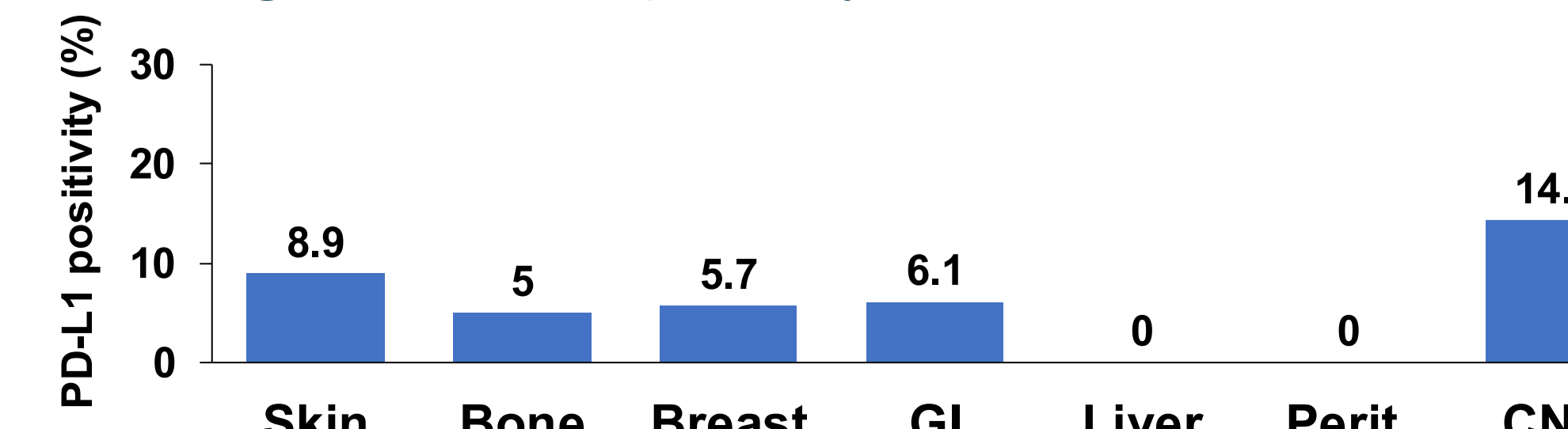


Figure 6. PD-L1 positivity ILC metastatic site



LND: Lymph nodes; Perit: peritoneum; CNS: central nervous system; GYN: female genital tract.

Immune Cell Infiltration

- Immune cell infiltration demonstrated organ-specific heterogeneity across metastatic sites in both ILC (Figure 7) and BC-NST (Figure 8), with significant differences observed in B cells, macrophage subsets (M1/M2), neutrophils, NK cells, dendritic cells, CD8+ T cells, and Tregs (all $q < 0.05$). CD4+ T-cell differences were observed only in BC-NST ($q = 0.002$).
- Liver and CNS metastases demonstrated relatively low immune infiltration, particularly in ILC, with low infiltration across multiple immune populations, including macrophage M2, Tregs, and CD8+ T cells. CNS metastases in both histologies showed especially low T-cell infiltration.

Figure 7. Immune cell infiltration in ILC metastatic site

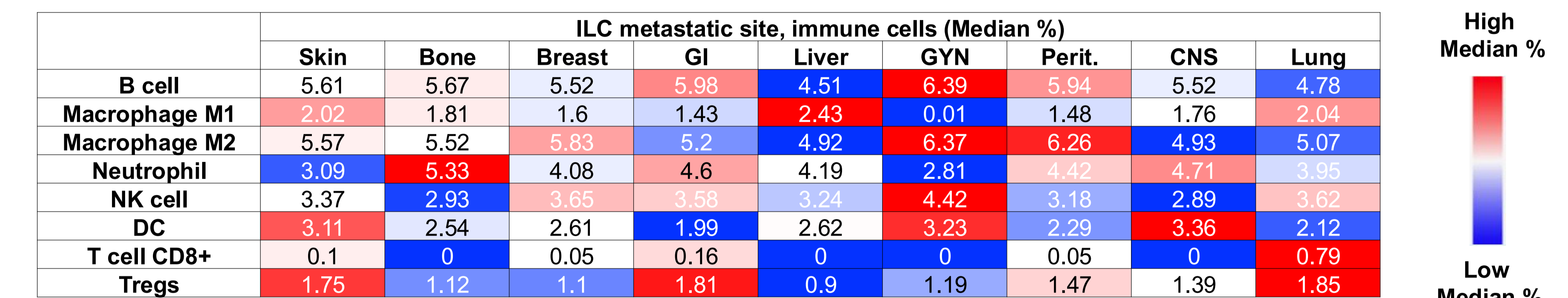
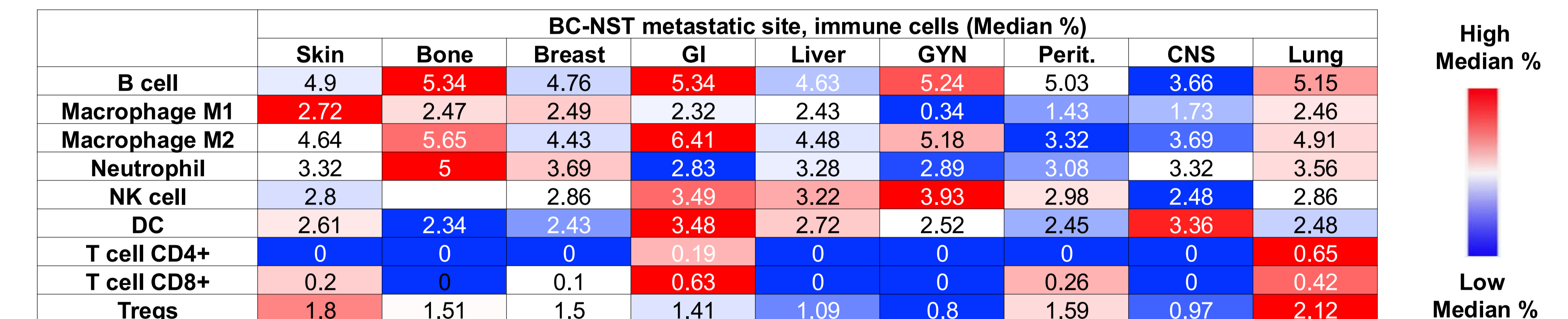


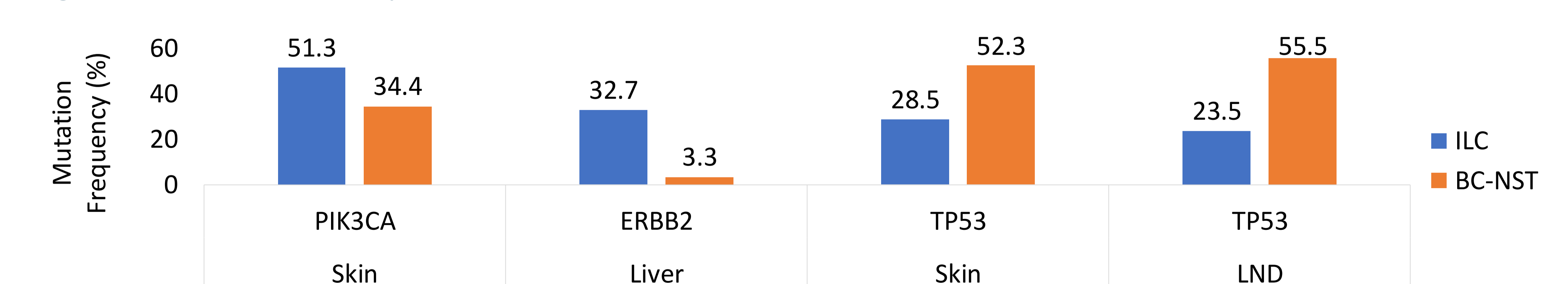
Figure 8. Immune cell infiltration in BC-NST metastatic site



Mutation among ILC vs BC-NST

- In organ-specific ILC vs BC-NST comparisons, *CDH1* mut were more frequent in ILC across sites, along with higher *PIK3CA* mut in skin (ILC 51.3% vs BC-NST 34.4%) and higher *ERBB2* mut in liver metastases (32.7% vs 3.3%), whereas a higher *TP53* mut frequency was observed in BC-NST in skin/soft tissue (28.5% vs 52.3%) and lymph nodes (23.5% vs 55.5%) (all $q < 0.01$) (Figure 9).

Figure 9. Mutation Frequency ILC vs BC-NST



CONCLUSIONS

- Metastatic BC exhibits marked organ-specific molecular and immune heterogeneity that differs by histology.
- These findings support histology- and site-aware interpretation of metastatic biopsies and may inform biomarker assessment and therapeutic decision-making in advanced disease.

CORRESPONDING AUTHOR:

Guilherme Nader-Marta, MD
 Contact: guilherme_nademarta@dfci.harvard.edu
 @GuiNaderMarta

References: 1. Raghavendra et al. JAMA Network Open. 2025; 2. Oesterreich S et al. JNCI 2022; 3. Onkar et al. Nat Cancer 2023

